

Transversity and T-odd PDFs from Drell-Yan processes with pp , pD and DD collisions

A. Sissakian¹, O. Shevchenko², A. Nagaytsev³, O. Ivanov⁴
Joint Institute for Nuclear Research, 141980 Dubna, Russia

Abstract

We estimate the single-spin asymmetries (SSA) which provide the access to transversity as well as to Boer-Mulders and Sivers PDFs via investigation of the single-polarized Drell-Yan (DY) processes with pp , pD and DD collisions available to RHIC, NICA, COMPASS, and J-PARC. The feasibility of these SSA is studied with the new generator of polarized DY events. The performed estimations demonstrate that there exist the such kinematical regions where SSA are presumably measurable. The most useful for PDFs extraction are the limiting kinematical ranges, where one can neglect the sea PDFs contributions which occur at large values of Bjorken x . It is of interest that on the contrary to the Sivers PDF, the transversity PDF is presumably accessible only in the especial kinematical region. On the contrary to the option with the symmetric collider mode (RHIC, NICA), this is of importance for the COMPASS experiment and the future J-PARC facility where the fixed target mode is available.

PACS: 13.65.Ni, 13.60.Hb, 13.88.+e

1 Introduction

In this paper we focus on DY processes in collisions of transversely polarized protons and deuterons, providing us an access to the very important and still poorly known sea and valence transversity, Boer-Mulders and Sivers PDFs in proton. At present the such processes are available to RHIC [1]. Their studies are planned at J-PARC [2] facility and, in principle, are possible⁵ at COMPASS, where unpolarized proton beam and both polarized proton and deuteron targets are available. Besides, at present JINR starts the new NICA/MPD project based on the development of the existing Nuclotron accelerator for the new facility creation: the heavy and light nucleus collider NICA [4], [5]. In particular, the possibility is now considered to study the collisions of the polarized proton and deuteron beams at the second interaction point (IP) at NICA. It is of importance, that all these experiments do not duplicate each other, but are complementary, providing us by the the information on the different PDFs measured in the different⁶ kinematical regions.

¹e-mail address: sisakian@jinr.ru

²e-mail address: shev@mail.cern.ch

³e-mail address: naga.jcev@sunse.jinr.ru

⁴e-mail address: ivon@jinr.ru

⁵At present the Drell-Yan program at COMPASS focuses on the pion-proton (deuteron) collisions (see, for example, [3]). However, the possibility to study DY processes with pp and pd collisions is now also under discussion.

⁶For pp collisions the center of mass energy is 200 GeV for RHIC. For COMPASS it can be varied from 20 to 27 GeV (upper bound corresponds to 400 GeV primary proton SPS beam). For J-PARC \sqrt{s} is planned to be about 8 GeV at first stage and about 10 GeV for the second stage. For NICA it is planned to be about 20-26 GeV.

The leading twist k_T integrated transversity PDF $\Delta_T q \equiv h_{1q}$, as well as the leading twist unpolarized $q \equiv f_{1q}$ and longitudinally polarized (helicity) $\Delta q \equiv g_{1q}$ PDFs, is of the crucial importance for understanding of the nucleon spin structure (see Ref. [6] for the comprehensive review). At the same time, nowadays the study of quark transverse momentum k_T dependent PDFs is also among the special issues in hadron physics. Of particular interest, are two leading-twist T-odd k_T dependent PDFs: Sivers function $f_{1T}^{\perp q}(x, k_T^2)$ and Boer-Mulders function $h_{1q}^{\perp}(x, k_T^2)$. While Sivers function represents the unpolarized parton distribution in a transversely polarized hadron, the Boer-Mulders function denotes the parton transversity distribution in the unpolarized hadron.

At present the Boer-Mulders PDF is still not measured, while the Sivers [7, 8] and transversity [9] PDFs were (preliminarily, with rather big uncertainties) extracted from the SIDIS data collected by HERMES [10] and COMPASS [11] collaborations. At the same time the analysis of SIDIS data suffers from the poor knowledge of the fragmentation functions, and especially it concerns the Collins fragmentation function which is necessary for the transversity extraction [9]. In this respect the Drell-Yan processes possess the essential advantage since they are free of any fragmentation functions. Besides, DY measurements *should* accompany SIDIS measurements to check the important QCD prediction [12] (see also [13] and references therein)

$$f_{1T}^{\perp}|_{DY} = -f_{1T}^{\perp}|_{SIDIS}, \quad h_1^{\perp}|_{DY} = -h_1^{\perp}|_{SIDIS} \quad (1)$$

for T-odd PDFs f_{1T}^{\perp} and h_1^{\perp} . It is relevant to notice in this connection that while the Sivers PDF was already extracted from SIDIS (with rather bad precision but at least the sign of $f_{1T}^{\perp}|_{SIDIS}$ is seen) there still was not the respective analysis for $h_1^{\perp}|_{SIDIS}$. Recently in the paper [14] the estimations were presented of the possibility to extract the azimuthal asymmetry $\langle \cos 2\phi \rangle$ (giving the access to h_1^{\perp}) from the combined analysis of all existing and planned SIDIS measurements. Thus, if this SIDIS program would be realized, then DY measurements can allow to check sign change effect for both Sivers and Boer-Mulders PDFs.

It is well known that the double transversely polarized DY process $H_1^{\uparrow} H_2^{\uparrow} \rightarrow l^+ l^- X$ allows to directly extract the transversity distributions (see Ref. [6] for review). However, at the same number of collected DY events, the double spin asymmetries suffer from the much more large statistical errors (product of the beam and target/beam polarizations in the denominator) than the single spin asymmetries. This is especially important for the double-polarized DY processes with pp (as well as with pD and DD) collisions, where because of the small value of transversity PDF for the sea antiquark in proton (neutron), the double spin asymmetry is estimated to be a few percents *maximum* [15]. Thus, in the case of pp , pD and DD collisions we focus on here, the double polarized DY processes seem to be not too useful and we need an alternative possibility allowing to extract the transversity PDF from the combined analysis of unpolarized

$$H_1 H_2 \rightarrow l^+ l^- X, \quad (2)$$

and single-polarized

$$H_1 H_2^{\uparrow} \rightarrow l^+ l^- X \quad (3)$$

DY processes. Besides, namely unpolarized and single-polarized DY processes give us also an access to Boers-Mulders and Sivers PDFs, which are very intriguing and interesting objects in themselves. On the other hand, in the processes (2) and (3) the access to PDFs we are interesting in is rather difficult since they enter the respective cross-sections [16] in the complex

convolution with each other, so that at first sight it is impossible to avoid some models on the k_T dependence of PDFs. To solve this problem the q_T weighting approach [17, 18, 19, 20] was recently applied in Ref. [7] to Sivers effect in the single-polarized DY processes (3), and in Refs. [21, 22] with respect to transversity and Boer-Mulders PDF extraction from both unpolarized and single-polarized DY processes (2) and (3). In two last cited papers we considered the DY processes with antiproton-proton and pion-proton collisions. At the same time the DY processes with the proton (deuteron)-proton(deuteron) collisions are also very important since they provide the access to sea PDFs. Within this paper we will estimate both types of single-spin asymmetries (SSA), which give us respectively access to Sivers PDF [7, 8] and to transversity and Boer-Mulders PDFs [21, 22]. At first sight it seems that DY processes with proton(deuteron)-proton(deuteron) collisions are strongly suppressed because there is no valence antiquark in the initial state there. However, we will see that there exist the kinematical regions where both SSA take quite considerable values.

2 Transversity and T-odd PDFs via Drell-Yan processes with pp collisions

The procedure proposed in Refs. [21, 22] allows us to extract from the processes (2) and (3) the transversity h_1 and the first moment

$$h_{1q}^{\perp(1)}(x) \equiv \int d^2\mathbf{k}_T \left(\frac{\mathbf{k}_T^2}{2M_p^2} \right) h_{1q}^{\perp}(x_p, \mathbf{k}_T^2) \quad (4)$$

of Boer-Mulders $h_1^{\perp(1)}$ PDF directly, without any model assumptions about k_T -dependence of $h_1^{\perp}(x, k_T^2)$. Applied to unpolarized DY process (2) with pp collisions this general procedure gives⁷

$$\hat{k} \Big|_{pp \rightarrow l+l^-X} = 8 \frac{\sum_q e_q^2 [\bar{h}_{1q}^{\perp(1)}(x_1) h_{1q}^{\perp(1)}(x_2) + (q \rightarrow \bar{q})]}{\sum_q e_q^2 [f_{1q}(x_1) f_{1q}(x_2) + (q \rightarrow \bar{q})]}, \quad (5)$$

where \hat{k} is the coefficient at $\cos 2\phi$ dependent part of the properly q_T weighted ratio of unpolarized cross-sections:

$$\hat{R} = \frac{\int d^2\mathbf{q}_T [|\mathbf{q}_T|^2/M_p^2] [d\sigma^{(0)}/d\Omega]}{\int d^2\mathbf{q}_T \sigma^{(0)}}, \quad (6)$$

$$\hat{R} = \frac{3}{16\pi} (\gamma(1 + \cos^2 \theta) + \hat{k} \cos 2\phi \sin^2 \theta). \quad (7)$$

At the same time, in the case of single-polarized DY process (3), operating just as in Ref. [21], one gets

$$\hat{A}_h = -\frac{1}{2} \frac{\sum_q e_q^2 [\bar{h}_{1q}^{\perp(1)}(x_p) h_{1q}(x_{p\uparrow}) + (q \rightarrow \bar{q})]}{\sum_q e_q^2 [\bar{f}_{1q}(x_p) f_{1q}(x_{p\uparrow}) + (q \rightarrow \bar{q})]}, \quad (8)$$

⁷Eq. (5) is obtained within the quark parton model. It is of importance that the large values of coefficient at $\cos 2\phi$ in the ratio of DY cross-sections can not be explained by the leading and next-to-leading order perturbative QCD corrections as well as by the high twists effects (see [16] and references therein).

where the single spin asymmetry (SSA) \hat{A}_h is defined as

$$\hat{A}_h = \frac{\int d\Omega d\phi_{S_2} \int d^2\mathbf{q}_T (|\mathbf{q}_T|/M_p) \sin(\phi + \phi_{S_2}) [d\sigma(\mathbf{S}_{2T}) - d\sigma(-\mathbf{S}_{2T})]}{\int d\Omega d\phi_{S_2} \int d^2\mathbf{q}_T [d\sigma(\mathbf{S}_{2T}) + d\sigma(-\mathbf{S}_{2T})]}. \quad (9)$$

All the notations used are the same as in Ref. [21] (see Ref. [6] for details on kinematics in the Collins-Soper frame we deal with).

Notice that SSA \hat{A}_h is analogous to asymmetry $A_{UT}^{\sin(\phi-\phi_S)\frac{q_T}{M_N}}$ (weighted with $\sin(\phi - \phi_S)$ and the same weight q_T/M_N) applied in Ref. [7] with respect to the Sivers effect investigation in the single-polarized DY processes. For DY process $pp^\uparrow \rightarrow l^+l^-X$ we study here the expressions for $A_{UT}^{\sin(\phi-\phi_S)\frac{q_T}{M_N}}$ look as (see Eqs. (14), (15) in Ref. [7])

$$A_{UT}^{\sin(\phi-\phi_S)\frac{q_T}{M_N}} = \frac{\int d\Omega d\phi_{S_2} \int d^2\mathbf{q}_T (|\mathbf{q}_T|/M_p) \sin(\phi - \phi_{S_2}) [d\sigma(\mathbf{S}_{2T}) - d\sigma(-\mathbf{S}_{2T})]}{\frac{1}{2} \int d\Omega d\phi_{S_2} \int d^2\mathbf{q}_T [d\sigma(\mathbf{S}_{2T}) + d\sigma(-\mathbf{S}_{2T})]}, \quad (10)$$

$$A_{UT}^{\sin(\phi-\phi_S)\frac{q_T}{M_N}} = 2 \frac{\sum_q e_q^2 [\bar{f}_{1T}^{\perp(1)q}(x_{p^\uparrow}) f_{1q}(x_p) + (q \rightarrow \bar{q})]}{\sum_q e_q^2 [f_{1q}(x_{p^\uparrow}) f_{1q}(x_p) + (q \rightarrow \bar{q})]}, \quad (11)$$

where

$$f_{1T}^{\perp(1)q}(x) \equiv \int d^2\mathbf{k}_T \left(\frac{\mathbf{k}_T^2}{2M_p^2} \right) f_{1T}^{\perp q}(x, \mathbf{k}_T^2) \quad (12)$$

is the first moment of the Sivers function $f_{1T}^{\perp q}(x, \mathbf{k}_T^2)$. Notice that factor 1/2 in denominator of Eq. (10) (see also Eq. (7) in Ref. [23]) was introduced in Ref. [7] (where the Sivers effect was studied in both SIDIS and DY processes) for consistence with the respective semi-inclusive SSA studied by the HERMES – see [8] and references therein. Since within this paper we also will study SSA given by Eqs. (10) and (11), for comparison purposes it is convenient to introduce⁸, by analogy, SSA

$$A_{UT}^{\sin(\phi+\phi_S)\frac{q_T}{M_N}} = 2\hat{A}_h = - \frac{\sum_q e_q^2 [\bar{h}_{1q}^{\perp(1)}(x_p) h_{1q}(x_{p^\uparrow}) + (q \rightarrow \bar{q})]}{\sum_q e_q^2 [f_{1q}(x_p) f_{1q}(x_{p^\uparrow}) + (q \rightarrow \bar{q})]}. \quad (13)$$

Let us now consider SSA given by Eqs. (11) and (13). On the contrary to valence PDFs, the sea PDFs dominate at small x and rapidly die out when x increases. That is why in the case of pp^\uparrow collisions we deal with the regions are of importance where the Bjorken x for sea PDFs take the small values, while, by virtue of the relation

$$x_p x_{p^\uparrow} = Q^2/s, \quad (14)$$

the valence PDFs occur at large x values. Indeed, in such the regions we can neglect the contributions to SSA containing sea PDFs at large x (later we will see that this is really good approximation) and, thereby, to essentially cancel the number of extra unknown PDFs entering the asymmetries.

⁸ Certainly, from the practical point of view, the such rescaling is not especially useful: when the asymmetry is multiplied by a number the error is multiplied by the same number too. However, it is convenient to consider both studied SSA given in the same scale in order to estimate and compare their feasibility at the same statistics of DY events.

Thus, let us consider two limiting cases $x_p \gg x_{p\uparrow}$ and $x_p \ll x_{p\uparrow}$. In the first case

$$x_{unpol} \gg x_{pol}, \quad (15)$$

neglecting⁹ the terms containing the sea PDFs at large x_p , one arrives at the simplified equations

$$A_{UT}^{\sin(\phi-\phi_S)\frac{q_T}{M_N}} \Big|_{x_p \gg x_{p\uparrow}} \simeq 2 \frac{4\bar{f}_{1T}^{\perp(1)u}(x_{p\uparrow})f_{1u}(x_p) + \bar{f}_{1T}^{\perp(1)d}(x_{p\uparrow})f_{1d}(x_p)}{4\bar{f}_{1u}(x_{p\uparrow})f_{1u}(x_p) + \bar{f}_{1d}(x_{p\uparrow})f_{1d}(x_p)}, \quad (16)$$

and

$$A_{UT}^{\sin(\phi+\phi_S)\frac{q_T}{M_N}} \Big|_{x_p \gg x_{p\uparrow}} \simeq -\frac{4h_{1u}^{\perp(1)}(x_p)\bar{h}_{1u}(x_{p\uparrow}) + h_{1d}^{\perp(1)}(x_p)\bar{h}_{1d}(x_{p\uparrow})}{4f_{1u}(x_p)\bar{f}_{1u}(x_{p\uparrow}) + f_{1d}(x_p)\bar{f}_{1d}(x_{p\uparrow})}. \quad (17)$$

Then, taking into account the quark charges and u quark dominance at large x , Eqs. (16) and (17) are essentially given by

$$A_{UT}^{\sin(\phi-\phi_S)\frac{q_T}{M_N}} \Big|_{x_p \gg x_{p\uparrow}} \simeq 2 \frac{\bar{f}_{1T}^{\perp(1)u}(x_{p\uparrow})f_{1u}(x_p)}{f_{1u}(x_{p\uparrow})f_{1u}(x_p)} = 2 \frac{\bar{f}_{1T}^{\perp(1)u}(x_{p\uparrow})}{f_{1u}(x_{p\uparrow})}, \quad (18)$$

and

$$A_{UT}^{\sin(\phi+\phi_S)\frac{q_T}{M_N}} \Big|_{x_p \gg x_{p\uparrow}} \simeq -\frac{h_{1u}^{\perp(1)}(x_p)\bar{h}_{1u}(x_{p\uparrow})}{f_{1u}(x_p)f_{1u}(x_{p\uparrow})}. \quad (19)$$

Analogously, in the second limiting case

$$x_{unpol} \ll x_{pol}, \quad (20)$$

one gets

$$A_{UT}^{\sin(\phi-\phi_S)\frac{q_T}{M_N}} \Big|_{x_p \ll x_{p\uparrow}} \simeq 2 \frac{4f_{1T}^{\perp(1)u}(x_{p\uparrow})\bar{f}_{1u}(x_p) + f_{1T}^{\perp(1)d}(x_{p\uparrow})\bar{f}_{1d}(x_p)}{4f_{1u}(x_{p\uparrow})f_{1u}(x_p) + f_{1d}(x_{p\uparrow})f_{1d}(x_p)}, \quad (21)$$

and

$$A_{UT}^{\sin(\phi+\phi_S)\frac{q_T}{M_N}} \Big|_{x_p \ll x_{p\uparrow}} \simeq -\frac{4\bar{h}_{1u}^{\perp(1)}(x_p)h_{1u}(x_{p\uparrow}) + \bar{h}_{1d}^{\perp(1)}(x_p)h_{1d}(x_{p\uparrow})}{4f_{1u}(x_p)f_{1u}(x_{p\uparrow}) + f_{1d}(x_p)f_{1d}(x_{p\uparrow})}, \quad (22)$$

with d quark contributions, while

$$A_{UT}^{\sin(\phi-\phi_S)\frac{q_T}{M_N}} \Big|_{x_p \ll x_{p\uparrow}} \simeq 2 \frac{f_{1T}^{\perp(1)u}(x_{p\uparrow})\bar{f}_{1u}(x_p)}{f_{1u}(x_{p\uparrow})f_{1u}(x_p)} = 2 \frac{f_{1T}^{\perp(1)u}(x_{p\uparrow})}{f_{1u}(x_{p\uparrow})}, \quad (23)$$

and

$$A_{UT}^{\sin(\phi+\phi_S)\frac{q_T}{M_N}} \Big|_{x_p \ll x_{p\uparrow}} \simeq -\frac{\bar{h}_{1u}^{\perp(1)}(x_p)h_{1u}(x_{p\uparrow})}{f_{1u}(x_p)f_{1u}(x_{p\uparrow})}, \quad (24)$$

⁹Notice that all over the paper we neglect in our calculations the contributions of strange PDFs which produce really tiny corrections.

neglecting d quark contribution.

Later (see Section 3) we will see that even the double approximations given by Eqs. (19) and (24) are in a very good agreement with Eqs. (11) and (13). It is of importance since allows us to cancel out the extra unknown variables entering the equations for measured asymmetries. In particular, this give us the interesting possibility to extract the ratios $h_{1u}/h_{1u}^{\perp(1)}$ and $\bar{h}_{1u}/\bar{h}_{1u}^{\perp(1)}$ directly, without application of the fitting procedure with a set of assumptions on extra unknown variables. Indeed, let us return to the unpolarized DY process with pp collisions, Eqs. (5)-(7). In the limiting cases $x_1 \gg x_2$ and $x_1 \ll x_2$ Eq. (5) is reduced to the equations

$$\hat{k}\Big|_{x_1 \gg x_2} \simeq 8 \frac{h_{1u}^{\perp(1)}(x_1) \bar{h}_{1u}^{\perp(1)}(x_2)}{f_{1u}(x_1) \bar{f}_{1u}(x_2)}, \quad (25)$$

and

$$\hat{k}\Big|_{x_1 \ll x_2} \simeq 8 \frac{\bar{h}_{1u}^{\perp(1)}(x_1) h_{1u}^{\perp(1)}(x_2)}{f_{1u}(x_1) \bar{f}_{1u}(x_2)}, \quad (26)$$

respectively. Then, having in our disposal the quantities $\hat{k}(x_1, x_2)$ and $\hat{A}_{UT}^{\sin(\phi+\phi_S) \frac{q_T}{M_N}}(x_p = x_1, x_{p\uparrow} = x_2)$ measured in unpolarized and single-polarized DY processes, and, combining Eqs. (19), (24) with Eqs. (25), (26), we can obtain the ratios $h_{1u}/h_{1u}^{\perp(1)}$ and $\bar{h}_{1u}/\bar{h}_{1u}^{\perp(1)}$ from the equations

$$\frac{\bar{h}_{1u}(x_1)}{\bar{h}_{1u}^{\perp(1)}(x_1)} \simeq -8 \frac{\hat{A}_{UT}^{\sin(\phi+\phi_S) \frac{q_T}{M_N}}}{\hat{k}} \Big|_{x_1 \gg x_2}, \quad \frac{h_{1u}(x_1)}{h_{1u}^{\perp(1)}(x_1)} \simeq -8 \frac{\hat{A}_{UT}^{\sin(\phi+\phi_S) \frac{q_T}{M_N}}}{\hat{k}} \Big|_{x_1 \ll x_2}. \quad (27)$$

3 Estimations on SSA in pp collisions

Let us first estimate SSA $A_{UT}^{\sin(\phi-\phi_S) \frac{q_T}{M_N}} \Big|_{pp\uparrow \rightarrow l+l-X}$ given by Eq. (11). Notice that for the RHIC kinematics SSA $A_{UT}^{\sin(\phi-\phi_S)}$ weighted only with the projecting factor $\sin(\phi - \phi_S)$ was already in detail studied in Ref. [23]. This asymmetry within the Gaussian model applied in [23] is just proportional to the q_T weighted SSA $A_{UT}^{\sin(\phi-\phi_S) \frac{q_T}{M_N}}$ which we consider in this paper: $A_{UT}^{\sin(\phi-\phi_S)} = a_{Gauss}^{DY} A_{UT}^{\sin(\phi-\phi_S) \frac{q_T}{M_N}}$ ($a_{Gauss}^{DY} \simeq 0.81 \cdot (1 \pm 10\%)$), so that we need not to repeat here the calculations for the RHIC kinematical domain. Instead, we present the estimations for the NICA kinematics, where two colliding $10 \sim 13 GeV$ proton beams assumed to be available [4], [5]. We perform the calculations for Q^2 values below and above J/Ψ threshold $Q^2 = 9.5 GeV^2$. For the estimations we use three different fits for the Siverts function: fits I and II from Ref. [7] and also the latest fit from Ref. [8], which we denote as fit III. These fits are given by the following parametrizations

$$\text{Fit I: } x f_{1T}^{\perp(1)u} = -x f_{1T}^{\perp(1)d} = 0.4x(1-x)^5, \quad (28)$$

$$\text{Fit II: } x f_{1T}^{\perp(1)u} = -x f_{1T}^{\perp(1)d} = 0.1x^{0.3}(1-x)^5, \quad (29)$$

$$\text{Fit III: } x f_{1T}^{\perp(1)u} = -x f_{1T}^{\perp(1)d} = (0.17...0.18)x^{0.66}(1-x)^5. \quad (30)$$

For the first moments (12) of the sea Siverts PDFs entering Eq. (11) we use the model (with the positive sign) proposed in Ref. [23] (see Eqs. (10) and (11) in Ref. [23]):

$$\frac{f_{1T}^{\perp(1)\bar{q}}(x)}{f_{1T}^{\perp(1)q}(x)} = \frac{f_{1\bar{u}}(x) + f_{1\bar{d}}(x)}{f_{1u}(x) + f_{1d}(x)} \quad (31)$$

For the unpolarized PDFs entering Eq. (11) we use GRV94 [24] parametrization. The results of estimations for the different Q^2 values are presented in Fig. 1.

Looking at Fig. 1 one can see that the asymmetry takes the largest values near zero value of $x_p - x_{p\uparrow}$ and when this difference becomes positive.

Notice that besides of parametrizations I, II and III on the Siverts PDF there exist also the parametrizations from Refs. [25], [26]. Our estimations¹⁰ with these parametrizations show that the values of $A_{UT}^{\sin(\phi-\phi_S)}$ are quite similar to the respective values obtained with the parametrizations I, II, III in the region $x_p > x_{p\uparrow}$ and even higher in the region $x_p < x_{p\uparrow}$. Thus, the prediction on $A_{UT}^{\sin(\phi-\phi_S)}$ with parametrizations I, II, III could be considered as even underestimated predictions: if $A_{UT}^{\sin(\phi-\phi_S)}$ predicted by parametrizations I, II, III will be seen within the errors, then the larger SSA predicted by the fits from Refs. [25] and [26] will be definitely measurable too.

Our calculations performed for the COMPASS and J-PARC kinematics (in comparison with RHIC rather close to the NICA one) produce for SSA $A_{UT}^{\sin(\phi-\phi_S)\frac{q_T}{M_N}}$ the plots very similar to the respective plots for the NICA kinematical range. The such behavior of $A_{UT}^{\sin(\phi-\phi_S)\frac{q_T}{M_N}}$ encourage one that it can be measured not only in the collider mode (RHIC, NICA) but also in the fixed target experiments (COMPASS, J-PARC). The point is that, as a rule, in the experiments with a fixed target the acceptance of the detector allows us to register mainly the events with the positive x_F :

$$x_F \equiv x_{beam} - x_{target} \gtrsim 0, \quad (32)$$

where x_{beam} and x_{target} are the Bjorken x values for the quarks inside of the beam and target protons, respectively. Thus, the option $x_p > x_{p\uparrow}$ can be realized by both COMPASS and J-PARC facilities, where unpolarized proton beam and polarized proton target can be available.

On the hand, the region $x_p < x_{p\uparrow}$, where SSA $A_{UT}^{\sin(\phi-\phi_S)\frac{q_T}{M_N}}$ is also quite considerable, definitely can be reached by the collider experiments RHIC and NICA, and, presumably, by J-PARC, where the option with the polarized beam is also planned (see Ref. [2]).

Let us now estimate SSA $A_{UT}^{\sin(\phi+\phi_S)\frac{q_T}{M_N}}$ given by Eq. (13). Since neither the Boer-Mulders function nor its first moment are still not measured, we will use in our calculation the Boer's model (Eq. (50) in Ref. [16]) which produces the good fit for the NA10 [28] and E615 [29] data on (anomalously large) $\cos(2\phi)$ dependence of DY cross-sections. This model gives for the first moment (4) entering Eq. (13) the value $h_{1q}^{\perp(1)}(x) \simeq 0.163f_1(x)$. We also apply the following assumption for the first moment of the sea Boer-Mulders PDF

$$\frac{h_{1\bar{q}}^{\perp(1)}(x)}{h_{1q}^{\perp(1)}(x)} = \frac{f_{1\bar{q}}(x)}{f_{1q}(x)}. \quad (33)$$

Notice that this assumptions is similar to the assumption (31), however, namely Eq. (33) is consistent with the Boer's model which we use here.

Recently, for the first time, the transversity PDF was extracted [9] from the combined data of HERMES [10], COMPASS [30] and BELLE [31] collaborations. However, because of the rather

¹⁰Dealing with the parametrization from Ref. [25] one should remember that the notations for Siverts PDF $\Delta^N f_{q/H\uparrow}$ and f_{1T}^{\perp} differ by the sign and extra multiplier: $f_{1T}^{\perp}(x, \mathbf{k}_T^2) = -(M/2|\mathbf{k}_T|)\Delta^N f_{q/H\uparrow}(x, \mathbf{k}_T^2)$ (see "Trento conventions" in Ref. [27]).

poor quality of data the error band surrounding the fit on h_1 is very large (see Fig. 2), and, besides, the authors of Ref. [9] were compelled to apply the large number of approximations. In particular, the approximation of zero sea transversity PDF was applied. However, as it was stressed before, in the case of proton-proton collisions namely the sea PDFs play the crucial role. That is why here we will apply two versions of evolution model for transversity instead of the fit from Ref. [9]. First is the model where the Soffer inequality is saturated [15]:

$$h_{1q}(x, Q_0^2) = \frac{1}{2} [q(x, Q_0^2) + \Delta q(x, Q_0^2)], \quad h_{1\bar{q}}(x, Q_0^2) = \frac{1}{2} [\bar{q}(x, Q_0^2) + \Delta \bar{q}(x, Q_0^2)] \quad (34)$$

at low initial scale ($Q_0^2 = 0.23 \text{ GeV}^2$), and then h_{1q} , $h_{1\bar{q}}$ are evolved with DGLAP. Certainly, this model rather gives the upper bound (maximal value) on SSA. In the second version of evolution model (see [6, 32] and references therein) the valence and sea transversity PDFs are assumed to be equal to helicity PDF Δq at the same initial scale (model scale) and then h_{1q} and $h_{1\bar{q}}$ are again evolved with DGLAP to the required Q^2 values. Certainly, this model is much more realistic one because at the model initial scale a lot of models predict [6] that $h_1 = \Delta q$. It is of importance that the curve corresponding to this version of evolution model lies just inside the error band for the fit of Ref. [9] – see Fig. 2. Thus, this version of evolution model is consistent with the analysis of Ref. [9].

We present here the estimations of SSA $A_{UT}^{\sin(\phi+\phi_S)\frac{q_T}{M_N}}$ below and above J/ψ resonance for the strongly different RHIC (Fig. 3) and NICA (Fig. 4) kinematical conditions. The respective plots for the COMPASS and J-PARC kinematics are again very similar to that for the NICA kinematical range.

Looking at Fig. 3 and 4 one can see that for both RHIC and NICA (as well as for COMPASS and J-PARC) kinematics the asymmetry $A_{UT}^{\sin(\phi+\phi_S)\frac{q_T}{M_N}}$ is negligible at $x_p > x_{p\uparrow}$ and is quite considerable at $x_p < x_{p\uparrow}$. In this second case SSA $A_{UT}^{\sin(\phi+\phi_S)\frac{q_T}{M_N}}$ takes its maximal values (about 5-10%) when $x_p - x_{p\uparrow}$ takes the large negative values. Thus, one can again see the advantage of the symmetric collider mode (RHIC, NICA) where the cases $x_p < x_{p\uparrow}$ and $x_p > x_{p\uparrow}$ do not differ especially. On the contrary, for the fixed target mode these cases essentially differ because of the acceptance restriction (32). Thus, to obtain nonzero $A_{UT}^{\sin(\phi+\phi_S)\frac{q_T}{M_N}}$ with the fixed target, one should either manage to avoid the restriction (32) dealing with unpolarized beam/polarized target option (forward-backward geometry spectrometer), or, in the case of the forward-geometry spectrometer (acceptance restriction (32) holds), one should deal with the polarized beam/unpolarized target option. Regretfully, both these options are hardly possible for the running COMPASS experiment. At the same time, the option with the polarized proton beam is now planned at J-PARC facility [2].

In conclusion of this section, let us estimate how good are the approximations given by Eqs. (16)-(19) in the case $x_p \gg x_{p\uparrow}$, and by Eqs. (21)-(24) in the case $x_p \ll x_{p\uparrow}$. This is very important for the analysis since these approximations allow us to cancel out the extra unknown variables entering the equations for measured asymmetries. The respective calculations of $A_{UT}^{\sin(\phi-\phi_S)\frac{q_T}{M_N}}$ are presented¹¹ by the Table 1. From this table it is seen that the approximations (16) and (21) obtained by neglecting the sea PDFs contributions at high x work very well (column “B”). At the same time, the agreement of the results obtained with the double approximations (18) and (23) (column “C”) with the result of column “A” is worse (but still

¹¹For better readability of the paper we present here only two tables for NICA kinematics. Our calculations show that for all another considered within the paper kinematical conditions the results are absolutely analogous.

Table 1: NICA kinematics. Values of $A_{UT}^{\sin(\phi-\phi_S)\frac{qT}{MN}}$ calculated by using Eq. (11) (labeled as A) in comparison with two approximations: Eqs. (16), (21), labeled as B, and Eqs. (18), (23), labeled as C. For f_{1T} the parametrization from Ref. [8] is used.

$s = 400 \text{ GeV}^2, Q^2 = 4 \text{ GeV}^2$				$s = 400 \text{ GeV}^2, Q^2 = 15 \text{ GeV}^2$			
$x_p - x_{p\uparrow}$	A	B	C	$x_p - x_{p\uparrow}$	A	B	C
-0.4000	0.0189	0.0184	0.0277	-0.4000	0.0178	0.0170	0.0277
-0.5000	0.0131	0.0129	0.0190	-0.5000	0.0132	0.0129	0.0204
-0.6000	0.0087	0.0086	0.0125	-0.6000	0.0093	0.0093	0.0142
-0.7000	0.0053	0.0053	0.0076	-0.7000	0.0061	0.0061	0.0091
-0.8000	0.0028	0.0028	0.0040	-0.8000	0.0033	0.0033	0.0049
0.4000	0.0514	0.0525	0.0614	0.4000	0.0828	0.0849	0.0984
0.5000	0.0486	0.0491	0.0556	0.5000	0.0811	0.0820	0.0922
0.6000	0.0460	0.0462	0.0509	0.6000	0.0788	0.0792	0.0867
0.7000	0.0437	0.0438	0.0471	0.7000	0.0764	0.0765	0.0818
0.8000	0.0417	0.0418	0.0439	0.8000	0.0742	0.0742	0.0775

not so bad). This is not surprising since in the applied parametrizations (28)-(30) for the Sivvers PDFs [7], [8] the relation $f_{1T}^{\perp(1)u} = -f_{1T}^{\perp(1)d}$ is used, which is argued within the $1/N_c$ expansion approach [33, 34].

On the other hand, in the case of asymmetry $A_{UT}^{\sin(\phi+\phi_S)\frac{qT}{MN}}$ both kinds of approximations (17), (19) and (22), (24) work very well (see Table 2).

Thus, dealing with the kinematical region $x_p \gg x_{p\uparrow}$ one can safely use the approximation (16) and, thereby, get the access to the first moments of the sea Sivvers PDFs. Dealing with the approximation (18) one should be more careful – if indeed $f_{1T}^{\perp(1)u} \simeq -f_{1T}^{\perp(1)d}$ then double approximation (18) is suitable only for some rather rough estimations. At the same time, we have no access to the transversity and Boer-Mulders function in the region $x_p \gg x_{p\uparrow}$ since the asymmetry $A_{UT}^{\sin(\phi+\phi_S)\frac{qT}{MN}}$ is negligible within this kinematical region. Let us recall that for the fixed target mode, this kinematical region corresponds to the option with the unpolarized beam and polarized target (if, certainly, we have in our disposal only the forward-geometry spectrometer – see Eq. (32)).

Let us now consider another limiting case $x_p \ll x_{p\uparrow}$, which in the case of the fixed target mode and forward-geometry spectrometer corresponds to the option with the polarized beam and unpolarized target. In this case the situation is absolutely opposite. Here the asymmetry $A_{UT}^{\sin(\phi+\phi_S)\frac{qT}{MN}}$ is quite considerable (and presumably is measurable as it was discussed above). As it has just shown, in this limit we can safely apply even double approximation (24). This give us the interesting possibility (see Section 2) to extract the ratio $h_{1u}/h_{1u}^{\perp(1)}$ directly, without application of fitting procedure with a set of assumptions on extra unknown variables.

4 SSA in pD and DD collisions

As usual, the inclusion of the deuteron beam/target can allow us to find PDFs of u and d quark, in separation.

Applying $SU_f(2)$ symmetry to the results of Section 3 one immediately gets the respective

Table 2: NICA kinematics. Values of $A_{UT}^{\sin(\phi+\phi_S)\frac{q_T}{M_N}}$ calculated by using Eq. (8) (labeled as A) in comparison with two approximations: (17), (22), labeled as B, and (19), (24), labeled as C. The evolution model for transversity with $h_{1q(\bar{q})} = \Delta q(\Delta \bar{q})$ at $Q_0^2 = 0.23 GeV^2$ is used.

$s = 400 GeV^2, Q^2 = 4 GeV^2$				$s = 400 GeV^2, Q^2 = 15 GeV^2$			
$x_p - x_{p\uparrow}$	A	B	C	$x_p - x_{p\uparrow}$	A	B	C
-0.4000	-0.0761	-0.0800	-0.0912	-0.4000	-0.0783	-0.0833	-0.0951
-0.5000	-0.0838	-0.0856	-0.0948	-0.5000	-0.0864	-0.0887	-0.0983
-0.6000	-0.0894	-0.0902	-0.0975	-0.6000	-0.0926	-0.0936	-0.1012
-0.7000	-0.0940	-0.0943	-0.1000	-0.7000	-0.0980	-0.0984	-0.1041
-0.8000	-0.0987	-0.0988	-0.1029	-0.8000	-0.1038	-0.1039	-0.1078
0.4000	0.0063	0.0067	0.0068	0.4000	0.0200	0.0216	0.0220
0.5000	0.0052	0.0054	0.0054	0.5000	0.0176	0.0184	0.0186
0.6000	0.0044	0.0045	0.0045	0.6000	0.0156	0.0159	0.0160
0.7000	0.0038	0.0038	0.0038	0.7000	0.0138	0.0139	0.0140
0.8000	0.0033	0.0033	0.0033	0.8000	0.0123	0.0124	0.0124

results on SSA for Drell-Yan processes in pD and DD collisions. For SSA giving an access to the Siverts PDF, in the limiting case (15) one gets instead of Eq. (16) the equations

$$A_{UT}^{\sin(\phi-\phi_S)\frac{q_T}{M_N}}(x_D \gg x_{p\uparrow}) \Big|_{Dp\uparrow \rightarrow l+l-X} \simeq 2 \frac{4\bar{f}_{1T}^{\perp(1)u}(x_{p\uparrow}) + \bar{f}_{1T}^{\perp(1)d}(x_{p\uparrow})}{4f_{1u}(x_{p\uparrow}) + f_{1d}(x_{p\uparrow})}, \quad (35)$$

and

$$\begin{aligned} A_{UT}^{\sin(\phi-\phi_S)\frac{q_T}{M_N}}(x_p \gg x_{D\uparrow}) \Big|_{pD\uparrow \rightarrow l+l-X} &= A_{UT}^{\sin(\phi-\phi_S)\frac{q_T}{M_N}}(x_D \gg x_{D\uparrow}) \Big|_{DD\uparrow \rightarrow l+l-X} \\ &\simeq 2 \frac{\bar{f}_{1T}^{\perp(1)u}(x_{D\uparrow}) + \bar{f}_{1T}^{\perp(1)d}(x_{D\uparrow})}{f_{1u}(x_{D\uparrow}) + f_{1d}(x_{D\uparrow})}, \end{aligned} \quad (36)$$

while in the limiting case (20) one obtains

$$A_{UT}^{\sin(\phi-\phi_S)\frac{q_T}{M_N}}(x_D \ll x_{p\uparrow}) \Big|_{Dp\uparrow \rightarrow l+l-X} \simeq 2 \frac{4f_{1T}^{\perp(1)u}(x_{p\uparrow}) + f_{1T}^{\perp(1)d}(x_{p\uparrow})}{4f_{1u}(x_{p\uparrow}) + f_{1d}(x_{p\uparrow})}, \quad (37)$$

and

$$\begin{aligned} A_{UT}^{\sin(\phi-\phi_S)\frac{q_T}{M_N}}(x_p \ll x_{D\uparrow}) \Big|_{pD\uparrow \rightarrow l+l-X} &= A_{UT}^{\sin(\phi-\phi_S)\frac{q_T}{M_N}}(x_D \ll x_{D\uparrow}) \Big|_{DD\uparrow \rightarrow l+l-X} \\ &\simeq 2 \frac{f_{1T}^{\perp(1)u}(x_{D\uparrow}) + f_{1T}^{\perp(1)d}(x_{D\uparrow})}{f_{1u}(x_{D\uparrow}) + f_{1d}(x_{D\uparrow})}. \end{aligned} \quad (38)$$

At the same time, SSA giving an access to transversity and Boer-Mulders PDFs look as

$$A_{UT}^{\sin(\phi+\phi_S)\frac{q_T}{M_N}}(x_D \gg x_{p\uparrow}) \Big|_{Dp\uparrow \rightarrow l+l-X} \simeq -\frac{[h_{1u}^{\perp(1)}(x_D) + h_{1d}^{\perp(1)}(x_D)][4\bar{h}_{1u}(x_{p\uparrow}) + \bar{h}_{1d}(x_{p\uparrow})]}{[f_{1u}(x_D) + f_{1d}(x_D)][4\bar{f}_{1u}(x_{p\uparrow}) + \bar{f}_{1d}(x_{p\uparrow})]}, \quad (39)$$

$$A_{UT}^{\sin(\phi+\phi_S)\frac{q_T}{M_N}}(x_p \gg x_{D\uparrow}) \Big|_{pD\uparrow \rightarrow l+l-X} \simeq -\frac{[4h_{1u}^{\perp(1)}(x_p) + h_{1d}^{\perp(1)}(x_p)][\bar{h}_{1u}(x_{D\uparrow}) + \bar{h}_{1d}(x_{D\uparrow})]}{[4f_{1u}(x_p) + f_{1d}(x_p)][\bar{f}_{1u}(x_{D\uparrow}) + \bar{f}_{1d}(x_{D\uparrow})]}, \quad (40)$$

and

$$A_{UT}^{\sin(\phi+\phi_S)\frac{qT}{MN}}(x_D \gg x_{D^\dagger}) \Big|_{DD^\dagger \rightarrow l+l-X} \simeq -\frac{[h_{1u}^{\perp(1)}(x_D) + h_{1d}^{\perp(1)}(x_D)][\bar{h}_{1u}(x_{D^\dagger}) + \bar{h}_{1d}(x_{D^\dagger})]}{[f_{1u}(x_D) + f_{1d}(x_D)][\bar{f}_{1u}(x_{D^\dagger}) + \bar{f}_{1d}(x_{D^\dagger})]} \quad (41)$$

in the limiting case (15), while

$$A_{UT}^{\sin(\phi+\phi_S)\frac{qT}{MN}}(x_D \ll x_{p^\dagger}) \Big|_{Dp^\dagger \rightarrow l+l-X} \simeq -\frac{[\bar{h}_{1u}^{\perp(1)}(x_D) + \bar{h}_{1d}^{\perp(1)}(x_D)][4h_{1u}(x_{p^\dagger}) + h_{1d}(x_{p^\dagger})]}{[f_{1u}(x_D) + f_{1d}(x_D)][4f_{1u}(x_{p^\dagger}) + f_{1d}(x_{p^\dagger})]}, \quad (42)$$

$$A_{UT}^{\sin(\phi+\phi_S)\frac{qT}{MN}}(x_p \ll x_{D^\dagger}) \Big|_{pD^\dagger \rightarrow l+l-X} \simeq -\frac{[4\bar{h}_{1u}^{\perp(1)}(x_p) + \bar{h}_{1d}^{\perp(1)}(x_p)][h_{1u}(x_{D^\dagger}) + h_{1d}(x_{D^\dagger})]}{[4\bar{f}_{1u}(x_p) + \bar{f}_{1d}(x_p)][f_{1u}(x_{D^\dagger}) + f_{1d}(x_{D^\dagger})]}, \quad (43)$$

and

$$A_{UT}^{\sin(\phi+\phi_S)\frac{qT}{MN}}(x_D \ll x_{D^\dagger}) \Big|_{DD^\dagger \rightarrow l+l-X} \simeq -\frac{[\bar{h}_{1u}^{\perp(1)}(x_D) + \bar{h}_{1d}^{\perp(1)}(x_D)][h_{1u}(x_{D^\dagger}) + h_{1d}(x_{D^\dagger})]}{[\bar{f}_{1u}(x_D) + \bar{f}_{1d}(x_D)][f_{1u}(x_{D^\dagger}) + f_{1d}(x_{D^\dagger})]} \quad (44)$$

in the limiting case (20).

As it was mentioned above (see Section 3) there exist the strong theoretical arguments [33], [34] based on $1/N_c$ expansion that the sum of the u and d quark Sivers first moments $f_{1T}^{\perp(1)u}$ and $f_{1T}^{\perp(1)d}$ is also very small quantity¹². Besides, the QCD evolution predicts small values of the sea transversity distributions *even at small x* values [32]. Thus, in the case of polarized deuteron in initial state, almost all respective SSA (see (36), (38), (40), (41)) presumably should be very small quantities (and our calculations confirm it), compatible with zero within the errors (certainly, it should be carefully checked by the respective measurements at RHIC, NICA, COMPASS and J-PARC). The only SSA which could take considerable value are SSA containing the sum $h_{1u}(x_{D^\dagger}) + h_{1d}(x_{D^\dagger})$ (see Eqs. (43), (44)). The point is that the analysis [9] of the COMPASS data [30] obtained on the deuteron target produced the possibility of nonzero sum $h_{1u} + h_{1d}$. In accordance with this analysis h_{1u} and h_{1d} are of opposite sign but differ¹³ in their absolute values (see Fig. 7 in Ref. [9]). However, the uncertainties on h_{1u} and h_{1d} are too large (see the error bands in Fig. 7) to realize is the quantity $h_{1u} + h_{1d}$ zero or not. Thus, the respective measurements of SSA in DY processes with polarized deuteron could shed the light on this problem.

On the contrary to the case of polarized deuteron, in the case of polarized proton all SSA could take the considerable values. Our calculations show that they are of the same order of magnitude as the respective SSA in the case of pp^\dagger collisions – see Figs 5, 6. Notice that for brevity we present the relations between SSA for pp^\dagger and Dp^\dagger collisions only for NICA since they are very similar (practically the same) to that for RHIC, COMPASS and J-PARC kinematics. In Fig. 5 we present the ratio $R = A_{UT}^{\sin(\phi-\phi_S)\frac{qT}{MN}} \Big|_{Dp^\dagger} / A_{UT}^{\sin(\phi-\phi_S)\frac{qT}{MN}} \Big|_{pp^\dagger}$. This ratio (which is the same for all three used parametrizations for Sivers function) changes from 0.4

¹²That is why the equality $f_{1T}^{\perp(1)u} + f_{1T}^{\perp(1)d} = 0$ in the parametrizations (28)-(30) is applied. Together with the assumption (31) it denotes that the equality $\bar{f}_{1T}^{\perp(1)u} + \bar{f}_{1T}^{\perp(1)d} = 0$ for the sea PDFs is also holds for these parametrizations.

¹³Evolution model, which is consistent with the analysis of Ref. [9] (see discussion around Fig. 2), also predicts that $h_{1u} \neq h_{1d}$.

to 0.8. In Fig. 6 we present the asymmetry $A_{UT}^{\sin(\phi+\phi_S)\frac{q_T}{M_N}}$ for Dp^\uparrow and pp^\uparrow collisions and it is seen that the respective curves almost merge. Thus, one can conclude that in the case of Dp^\uparrow collisions both, weighted with $\sin(\phi - \phi_S)$ and weighted with $\sin(\phi + \phi_S)$, SSA are presumably measurable in the same x regions as the respective SSA in the case of pp^\uparrow collisions.

5 Estimations on the SSA feasibility with the new generator of polarized DY events

Generator of polarized Drell-Yan events is necessary for *first*, estimation of the SSA feasibility on the preliminary (theoretical) stage (without details of experimental setup) – just this paper. *Second*, as an input for detector simulation software (for example, GEANT [35] based code) on both planning of experimental setup and the data analysis stages. Until recently there was no in the free access any generator of Drell-Yan events except for the only PYTHIA generator [36]. However, regretfully, in PYTHIA there are only unpolarized Drell-Yan processes and, besides, they are implemented in PYTHIA without correct q_T and $\cos 2\phi$ dependence, which is absolutely necessary to study Boer-Mulders effect. Recently did appear the first generator of polarized DY events [37], [38] where q_T and angle dependencies are properly taken into account.

To simplify implementation of the new possibilities in program and to effectively control all calculations we wrote the new generator of polarized DY events (the details will be published elsewhere). The scheme of generator is quite simple and very similar to the event generator GMC_TRANS [39] which was successfully used by HERMES collaboration for simulation of the Sivers effect in semi-inclusive DIS processes [40]. Briefly, the scheme of DY event generation look as follows. First, the generator performs the choice of flavor q of annihilating $q\bar{q}$ pair and choice does the given hadron (for example, polarized) contains annihilating quark or, alternatively, antiquark of given (chosen) flavor. It is done in accordance with the total unpolarized DY cross-sections for each flavor and each alternative choice for given hadron in initial state (annihilating quark or antiquark inside). Then, the variables x_F and Q^2 are selected according to the part of unpolarized cross-section (see, for example, Eq. (1) in Ref. [21]) which does not contain the angle dependencies. At the next step the polar angle θ is selected from $\sin\theta(1 + \cos^2\theta)$ distribution in that cross-section. Then, the Gaussian model for $f_{1q}(x, k_T)$ is applied and after that the transverse momentum of lepton pair q_T is selected from exponential distribution $\exp(-q_T^2/2)/2\pi$. At the next step ϕ and ϕ_S angles are selected in accordance with $\cos 2\phi$, $\sin(\phi - \phi_S)$ and $\sin(\phi + \phi_S)$ dependencies of the single-polarized DY cross-section (see, for example, Eq. (2) in Ref. [21]). The k_T dependencies of Boer-Mulders $h_{1q}^\perp(x, k_T)$ and Sivers $f_{1T}^q(x, k_T)$ PDFs are fixed by the Boer model [16] and Gaussian ansatz [7, 8], respectively. At this stage of ϕ and ϕ_S selection x_F , Q^2 , θ and q_T variables are already fixed¹⁴ that essentially increases the rate of ϕ and ϕ_S selection. All variables are generated using the standard von Neumann acceptance-rejection technique (see, for example [36]).

Let us stress once again that the generator elaborated in [37, 38] is the first generator of polarized DY events and in many respects it helped us to construct our generator. Now we briefly consider the advantages of the new generator. As it was discussed above, one of the main requirement to any generator of polarized DY events is to properly include the nontrivial q_T dependence of DY cross-sections. This is of especial importance for the q_T weighted objects

¹⁴Certainly, one can select all variables simultaneously. However, such scheme essentially decreases the rate of events generation.

we deal with in the paper. In the earlier generator [37, 38] the approximations are applied for the convolution calculations in the h_{1q}^\perp containing parts of DY cross-section just as it was done in the original paper [16] (see the discussion around Eqs. (47) and (53) in Ref. [16]). However, the direct calculations show that implementation of these approximation in the generator leads to essential distortion of the q_T weighted objects, such as SSA $A_{UT}^{\sin(\phi+\phi_S)\frac{q_T}{M_N}}$: the values of SSA obtained from simulated data significantly differ from the respective values calculated directly from the input parametrizations/models for f_{1q} , $h_{1q}^{\perp(1)}$ and h_{1q} . That is why we avoid the such kind of approximations. Instead, we calculate the convolutions numerically for the large discrete set of q_T values and then we perform the standard spline interpolation procedure to reconstruct the calculated convolution as the continuous function of q_T . As a result (see Figs. 7-10 below), the values of SSA $A_{UT}^{\sin(\phi+\phi_S)\frac{q_T}{M_N}}$ reconstructed from simulated data are in a good agreement with the respective values calculated directly from the parametrizations/models entering the generator as an input.

Another advantage of the new generator is that it can be much more easy combined¹⁵ with the PYTHIA generator (where almost all possible processes are included) which is necessary for the analysis of background processes that can produce false DY events (misidentification of lepton pair). The point is that, on the contrary to generator [37, 38], in our generator, just as in PYTHIA, the DY processes are generated for each flavor in separation. Besides, the constructed generator have some technical advantages: due to the chosen generation scheme the rate of event generation is much higher than for generator [37, 38], where all kinematical variables are thrown simultaneously; the search for cross-sections maximums for the von Neumann algorithm is performed automatically as well as the calculation of the total cross-section at the end of each generation run.

Having in our disposal the generator of polarized DY events, we can now estimate the feasibility of SSA calculated before. Certainly, these are very preliminary estimations on the first (theoretical level). To perform the comprehensive feasibility estimations one needs to take into account the all peculiarities of the concrete experimental setup.

We prepared two samples with applied statistics 100K and 50K of pure Drell-Yan events for each of two Q^2 ranges: $2 < Q^2 < 8.5 \text{ GeV}^2$ and $Q^2 > 11 \text{ GeV}^2$. Cut $2 < Q^2 < 8.5 \text{ GeV}^2$ is applied to avoid misidentification of lepton pairs due to numerous background processes (combinatorial background from Dalitz-decays and gamma conversions, etc – see, for instance, section F.4.2 in Ref. [41]) below $Q^2 = 2 \text{ GeV}^2$ and to exclude lepton pairs coming from J/ψ region. Cut $Q^2 > 11 \text{ GeV}^2$ is also applied to avoid the lepton pairs coming from J/ψ region.

As before, we did not present here the estimation on feasibility of $A_{UT}^{\sin(\phi-\phi_S)\frac{q_T}{M_N}} \Big|_{pp^\uparrow}$ for RHIC kinematics because it was in detail done in Ref. [8]. So, for this SSA we again (see Section 3) present here the results only for the NICA center of mass energy 20 GeV having in mind that the results on SSA for COMPASS and J-PARC (in comparison with RHIC rather close in \sqrt{s} to NICA) occur quite similar (see Section 3) to the respective results for NICA. The results are presented in Fig. 7. For the simulations with the developed generator we use the latest parametrization, fit III (solid line in Fig. 7), from the set (28)-(30). Looking at Fig. 7 one can see that even at relatively low applied statistics 50K pure Drell-Yan events (bottom part of Fig. 7) there are three presumably measurable points for $A_{UT}^{\sin(\phi-\phi_S)\frac{q_T}{M_N}}$ in the kinematical region $x_p - x_{p^\uparrow} > 0$, where this SSA is about 4-6%. Moreover, at applied statistics 100K pure Drell-

¹⁵This work now in progress.

Yan events one can hope to reconstruct the functional form of SSA $A_{UT}^{\sin(\phi-\phi_S)\frac{q_T}{M_N}}$ (see top part of Fig. 7) in the kinematical region $x_p > x_{p\uparrow}$. Since kinematical region $x_p > x_{p\uparrow}$ corresponds to $x_F > 0$ for the fixed target mode with unpolarized beam and polarized target available to COMPASS and J-PARC, one can conclude that all four RHIC, NICA, COMPASS and J-PARC facilities can provide us the access to the Sivvers PDF (see Section 3). In the region $x_p < x_{p\uparrow}$ available to RHIC, NICA and (presumably) J-PARC, SSA $A_{UT}^{\sin(\phi-\phi_S)\frac{q_T}{M_N}}$ is smaller (less than 4%), but still visible within the errors (even at applied statistics 50K events one can see at least one measurable point).

Let us now consider feasibility of the Sivvers PDFs in the case of the deuteron in initial state. Looking at Figs. 5 and 7 one can conclude that the only SSA $A_{UT}^{\sin(\phi-\phi_S)\frac{q_T}{M_N}}|_{Dp\uparrow}$ which could take considerable values (see Section 4) is hardly measurable at applied statistics 50K pure Drell-Yan events. At the same time, in the case of 100K events this asymmetry becomes presumably measurable.

Let us now estimate the feasibility of SSA $A_{UT}^{\sin(\phi+\phi_S)\frac{q_T}{M_N}}$ giving us an access to transversity and Boer-Mulders PDFs. We again (see Section 3) present the estimations for $pp\uparrow$ collisions and for two quite different RHIC and NICA center of mass energies. The results are presented in Figs. 8 and 9. For COMPASS and J-PARC kinematics our calculations produce almost the same figures as for NICA center of mass energy, so that we again omit the respective plots. For the simulations with the developed generator we again use (see Section 3) Boer model for h_1^\perp and the evolution model for h_1 with $h_{1q(\bar{q})} = \Delta q(\Delta\bar{q})$ ansatz at initial scale $Q_0^2 = 0.23 \text{ GeV}^2$.

Looking at Figs. 8 and 9 one can see that in the region $x_p < x_{p\uparrow}$ even at statistics 50K pure Drell-Yan events (bottom part of Fig. 8) one can hope to see within the errors at least three points for $A_{UT}^{\sin(\phi+\phi_S)\frac{q_T}{M_N}}$ in the kinematical region $x_p - x_{p\uparrow} < 0$. At the same time, at the statistics 100K events one can hope also to reconstruct the functional form of this SSA (see top part of Fig. 8) in the kinematical region $x_p < x_{p\uparrow}$. Regretfully, the kinematical region $x_p < x_{p\uparrow}$ is hardly accessible for COMPASS because of the forward geometry spectrometer and the unpolarized proton beam available to this running experiment. In the case of another experiment with the fixed target, planning at J-PARC facility, one could reach this kinematical region if the polarized proton beam would be available (this option is now planned at J-PARC [2]). Fortunately, there are no any problems to reach the kinematical region $x_p < x_{p\uparrow}$ for the symmetric collider mode available to RHIC and NICA.

Let us note that due to the close values of $A_{UT}^{\sin(\phi+\phi_S)\frac{q_T}{M_N}}$ in the cases of $pp\uparrow$ and $Dp\uparrow$ collisions (see Fig. 6) all conclusions concerning feasibility of $A_{UT}^{\sin(\phi+\phi_S)\frac{q_T}{M_N}}$ in the case of $pp\uparrow$ collisions are valid in $Dp\uparrow$ case too.

Looking at Figs. 7-9 one can see that if the available experimental statistics will be rather low (less than 50K events) it is hardly possible to reconstruct the functional form of Sivvers and Boer-Mulders PDFs. However, even in this unfavorable case one can hope at least to check very important QCD prediction (1).

In conclusion of this section let us estimate the feasibility of both $A_{UT}^{\sin(\phi-\phi_S)\frac{q_T}{M_N}}$ and $A_{UT}^{\sin(\phi+\phi_S)\frac{q_T}{M_N}}$ SSA for the $\pi^- p\uparrow \rightarrow \mu^+ \mu^- X$ DY processes available to COMPASS. The model estimation of SSA $A_{UT}^{\sin(\phi+\phi_S)\frac{q_T}{M_N}}$ magnitude was already presented in the previous paper [22]. However, that time we could not present the feasibility estimations for this SSA because there still was not any generator of polarized DY events in the free access. Besides, only recently the optimal

kinematical conditions for DY program at COMPASS were chosen. These are the pion beam energy 160 GeV and the range $4 < Q < 9$ GeV for the invariant dilepton mass [3]. The results on SSA $A_{UT}^{\sin(\phi \pm \phi_S) \frac{qT}{MN}} \Big|_{\pi^- p^\uparrow}$ are presented in Fig. 10. Because of the restriction (32) for the COMPASS forward geometry spectrometer we present the results only for $x_\pi > x_{p^\uparrow}$. Looking at Fig. 10 one can see that even at rather low applied statistics 50K events there six presumably measurable points for both asymmetries, which encourage us that it could be possible to reconstruct the functional form for both SSA. Thus, one can conclude that for COMPASS it is much more profitable to study DY processes with the pion-proton collisions. At the same time, as it was discussed above, DY processes $p(D)p^\uparrow(D^\uparrow) \rightarrow l^+l^-X$ could be most successfully studied in collider mode at RHIC and NICA.

6 Conclusion

In summary, the Drell-Yan processes with the colliding protons and deuterons available to RHIC, NICA, COMPASS and J-PARC were considered. We estimated the single-spin asymmetries $A_{UT}^{\sin(\phi - \phi_S) \frac{qT}{MN}}$ and $A_{UT}^{\sin(\phi + \phi_S) \frac{qT}{MN}}$, which give us an access to Sivers and to Boer-Mulders and transversity PDFs, respectively. The estimations were performed for the different \sqrt{s} values, corresponding to the kinematical conditions of RHIC, NICA, J-PARC and COMPASS facilities.

The preliminary estimations for pp^\uparrow collisions demonstrate that SSA $A_{UT}^{\sin(\phi - \phi_S) \frac{qT}{MN}}$ can reach quite considerable values (5-10%) in both $x_p > x_{p^\uparrow}$ and $x_p < x_{p^\uparrow}$ regions. On other hand, the estimations performed for SSA $A_{UT}^{\sin(\phi + \phi_S) \frac{qT}{MN}}$ show that this asymmetry is negligible in the region $x_p > x_{p^\uparrow}$ and takes considerable values (also about 5-10%) in the region $x_p < x_{p^\uparrow}$. The estimations performed for SSA in the case of Dp and DD collisions demonstrate that the asymmetries for DY processes with pD^\uparrow collisions are compatible with zero except for perhaps one, containing sum $h_{1u} + h_{1d}$. The latest analysis [9] predicts that this sum could essentially differ from zero. Certainly, because of very large uncertainties, this is very preliminary conclusion which should be carefully checked in the future DY experiments. On the contrary to DY processes with pD^\uparrow and DD^\uparrow collisions, SSA for Dp^\uparrow collisions are close in their values to the respective SSA for pp^\uparrow collisions and, thus, presumably could be feasible in the same kinematical regions. While SSA $A_{UT}^{\sin(\phi - \phi_S) \frac{qT}{MN}} \Big|_{Dp^\uparrow}$ is about 50-80% of $A_{UT}^{\sin(\phi - \phi_S) \frac{qT}{MN}} \Big|_{pp^\uparrow}$, the asymmetry $A_{UT}^{\sin(\phi + \phi_S) \frac{qT}{MN}} \Big|_{Dp^\uparrow}$ is even slightly larger than $A_{UT}^{\sin(\phi + \phi_S) \frac{qT}{MN}} \Big|_{pp^\uparrow}$.

The new generator of polarized DY events was developed which allowed us to estimate the feasibility of both weighted with $\sin(\phi - \phi_S)$ and $\sin(\phi + \phi_S)$ single-spin asymmetries. These estimations performed for proton-proton collisions demonstrate that both SSA are presumably measurable even at the applied statistics 50K pure Drell-Yan events. While $A_{UT}^{\sin(\phi - \phi_S) \frac{qT}{MN}}$ is presumably measurable in both kinematical regions $x_p > x_{p^\uparrow}$ and $x_p < x_{p^\uparrow}$, the asymmetry $A_{UT}^{\sin(\phi + \phi_S) \frac{qT}{MN}}$ could be measured only in the region $x_p < x_{p^\uparrow}$, where it takes quite considerable values. It is of importance that while for the symmetric collider mode (RHIC, NICA) there is no any difficulties to reach both $x_p > x_{p^\uparrow}$ and $x_p < x_{p^\uparrow}$ kinematical regions, for the fixed target mode (COMPASS, J-PARC), there is the problem to reach the region $x_p < x_{p^\uparrow}$. This is hardly possible for the running COMPASS experiment, where only unpolarized proton beam and forward geometry spectrometer is available. At the same time it still could be achieved by

J-PARC, where at present the option with polarized proton beam is planned.

We also studied the behavior of SSA in two different limiting cases, $x_p \gg x_{p\uparrow}$ and $x_p \ll x_{p\uparrow}$. It is of importance that in these limiting cases one can essentially reduce the number of unknown PDFs entering the asymmetries. In particular, studying the unpolarized and single-polarized Drell-Yan processes in the limiting case $x_p \ll x_{p\uparrow}$ one can directly extract the ratio of transversity and first moment of Boer-Mulders PDF.

Thus, one can conclude that it is much better to study the single-polarized DY processes with pp , pD and DD collisions in the symmetric collider mode (RHIC and NICA). For fixed target experiments (like J-PARC and COMPASS) the polarized proton beam is necessary to improve the situation. This option is planned at J-PARC but is hardly possible for already running COMPASS experiment, where it is much more profitable to study DY processes with the pion-proton collisions (namely this option now is planned at COMPASS [3]).

Let us stress once again that any new measurements of SSA in Drell-Yan processes are of extreme importance even at rather poor available statistics of collected Drell-Yan events. Even in this unfavorable case one can at least to check very important QCD prediction (1), which would provide a crucial test of our understanding of T-odd effects within QCD and the factorization approach to the processes sensitive to transverse parton momenta. It is encouraging that today the Drell-Yan measurements are planned simultaneously in the different world centers for high energy physics.

Acknowledgments

The authors are grateful to R. Bertini, O. Denisov, A. Efremov, Y. Goto, T. Iwata, S. Kazutaka, V. Kekelidze, S. Kumano, A. Maggiora, I. Meshkov, A. Olshevsky, G. Piragino, G. Pontecorvo, S. Sawada, I. Savin, A. Sorin and O. Teryaev, for fruitful discussions.

The work of O. Shevchenko, A. Nagaytsev and O. Ivanov was supported by the Russian Foundation for Basic Research (Project No. 07-02-01046).

References

- [1] RHIC Spin Collab., D. Hill et al., letter of intent RHIC-SPIN-LOI-1991, updated 1993; G. Bunce et al., Particle World 3, 1 (1992); PHENIX/Spin Collaboration, K. Imai et al., BNL-PROPOSAL-R5-ADD (1994). O. Martin, A. Schafer, M. Stratmann, W. Vogelsang, Phys. Rev. D57 (1998) 3084; Phys. Rev. D60 (1999) 117502.
- [2] J. Chiba et al, J-PARC proposal “Measurement of high-mass dimuon production at the 50-GeV proton synchrotron”, can be obtained electronically via http://j-parc.jp/NuclPart/pac_0606/pdf/p04-Peng.pdf
- [3] M. Colantoni, talk given at Transversity 2008 workshop, May 28th - May 31st, 2008 Ferrara, Italy; accessible electronically via <http://www.fe.infn.it/transversity2008/>
- [4] A.Sissakian et al., Conceptual Design Report “Design and Construction of Nuclotron-based Ion Collider facility (NICA)”, Dubna 2007. Accessible electronically via http://nucloserv.jinr.ru/nica_webpage/Nica_files/reports/CDR_07/CDR_NICA%20.html
- [5] A.N. Sissakian, A.S. Sorin and V.D. Toneev, QCD Matter: A search for a mixed quark-hadron phase, nucl-th/0608032.

- [6] V. Barone, A. Drago, and P.G. Ratcliffe, Phys. Rep. **359**, 1 (2002).
- [7] A. V. Efremov et al, Phys. Lett. B612 (2005) 233
- [8] J.C. Collins et al, Phys. Rev. D73 (2006) 014021
- [9] M. Anselmino et al, Phys. Rev. D75 (2007) 054032
- [10] HERMES collaboration (A. Airapetian et al), Phys. Rev. Lett. **84**, 4047 (2000); Phys. Rev. D **64**, 097101 (2001); Phys. Lett. B **562**, 182 (2003); Phys. Rev. Lett. **94**, 012002 (2005).
- [11] E.S. Ageev et al (COMPASS collaboration), Nucl. Phys. B 765 (2007) 31
- [12] J. C. Collins, Phys. Lett. B 536 (2002) 43
- [13] J. Collins, Rapidity divergences and valid definitions of parton densities, Proceedings of LIGHT CONE 2008; eprint: arXiv:0808.2665v2 [hep-ph]
- [14] V. Barone, A. Prokudin, B.-Q. Ma, Phys. Rev. D78 (2008) 045022
- [15] O. Martin, A. Schäfer, M. Stratmann and W. Vogelsang, Phys. Rev. D57 (1998) 3084
- [16] D. Boer, Phys. Rev. D **60**, 014012 (1999)
- [17] A. Kotzinian, P.J. Mulders, Phys. Letts. B 406 (1997) 373.
- [18] D. Boer, R. Jakob, P. J. Mulders, Nucl. Phys. B **504**, 345 (1997)
- [19] D. Boer, R. Jakob, P. J. Mulders, Phys. Lett. B **424**, 143 (1998)
- [20] D. Boer, P. J. Mulders, Phys. Rev. D **57**, 5780 (1998)
- [21] A.N. Sissakian, O.Yu. Shevchenko, A.P. Nagaytsev, O.N. Ivanov, Phys. Rev. **D72** (2005) 054027
- [22] A. Sissakian, O. Shevchenko, A. Nagaytsev, O. Denisov, O. Ivanov Eur. Phys. J. C46 (2006) 147
- [23] J.C. Collins et al, Phys. Rev. D73 (2006) 094023
- [24] M. Gluck, E. Reya, A. Vogt, Z. Phys. C67 (1995) 433
- [25] M. Anselmino et al, Phys. Rev. D 72 (2005) 094007
- [26] W. Vogelsang, F. Yuan, Phys. Rev. D 72 (2005) 054028
- [27] A. Bacchetta, U. D'Alesio, M. Diehl, C. A. Miller, arXiv:hep-ph/0410050
- [28] NA10 Collab., Z. Phys. **C31**, 513 (1986);
- [29] J.S. Conway et al, Phys. Rev. **D39**, 92 (1989).
- [30] V. Y. Alexakhin, et al., Phys. Rev. Lett. 94, 202002 (2005), hep-ex/0503002.

- [31] Belle Collaboration, R. Seidl et al., Phys. Rev. Lett. 96, 232002 (2006).
- [32] V. Barone , T. Calarco, A. Drago, Phys. Rev. D56 (1997) 527
- [33] P.V. Pobylitsa, hep-ph/0301236
- [34] A. V. Efremov, K. Goeke and P. V. Pobylitsa, Phys. Lett. B 488 (2000) 182 [arXiv:hep-ph/0004196].
- [35] See <http://wwwasd.web.cern.ch/wwwasd/geant/>
- [36] T. Sjostrand et al., hep-ph/0308153.
- [37] A. Bianconi, M. Radici, Phys. Rev. D73 (2006) 034018; Phys. Rev. D72 (2005) 074013
- [38] A. Bianconi, arXiv:0806.0946 [hep-ex]
- [39] N.C.R. Makins, GMC_trans manual, HERMES internal report 2003, HERMES-03-060; G. Schnell, talk at workshop Transversity'07, ECT* Trento, Italy, June 2007
- [40] A. Airapetian et al. (HERMES Collaboration), Phys. Rev. Lett. 84, 4047 (2000); Phys. Rev. D 64, 097101 (2001); Phys. Lett. B 562, 182 (2003)
- [41] V. Barone et. al (PAX collaboration), hep-ex/0505054
- [42] M. Gluck, E. Reya, M. Stratmann, W. Vogelsang, Phys. Rev. D53 (1996) 4775
- [43] M. Gluck, E. Reya, A. Vogt, Z. Phys. C53 (1992) 651

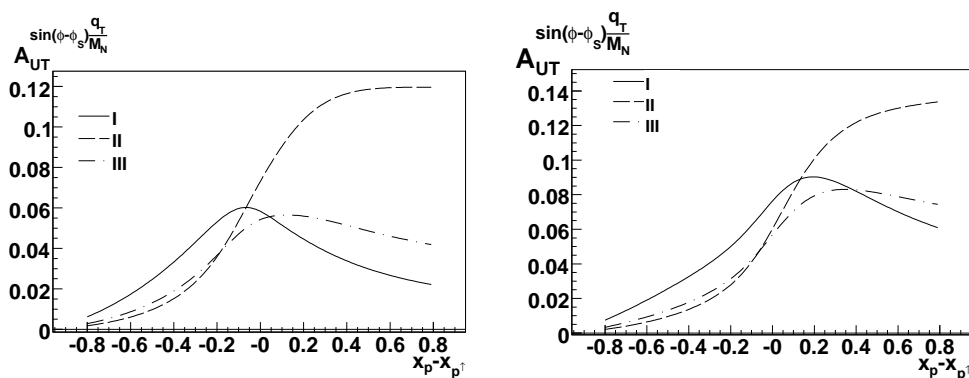


Figure 1: Estimation of SSA $A_{UT} \left. \frac{\sin(\phi-\phi_S) q_T}{M_N} \right|_{pp\uparrow}$ for NICA, $s=400 GeV^2$, with $Q^2 = 4 GeV^2$ (left) and $Q^2 = 15 GeV^2$ (right). Rome numbers I, II denote respectively fits I and II from Ref. [7] and III denotes the fit from Ref. [8].

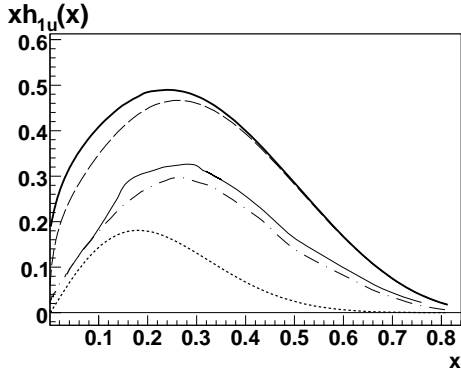


Figure 2: Results of Ref. [9] on h_{1u} in comparison with the results obtained with two versions of evolution model and with the Soffer bound. The bold solid line (top) corresponds to upper bound given by the Soffer inequality. Dashed line corresponds to the evolution model with the Soffer inequality saturation at the initial model scale $Q_0^2 = 0.23 \text{ GeV}^2$. The solid line corresponds to the upper boundary of the error band on h_{1u} . The dashed-dotted line corresponds to the evolution model, where $h_{1u,\bar{u}} = \Delta u(\Delta\bar{u})$ at initial scale $Q_0^2 = 0.23 \text{ GeV}^2$. The dotted line corresponds to the fit of Ref. [9] on h_{1u} . GRV94 [24] parametrization for $q(x)$ and GRSV95 [42] parametrization for $\Delta q(x)$ are used.

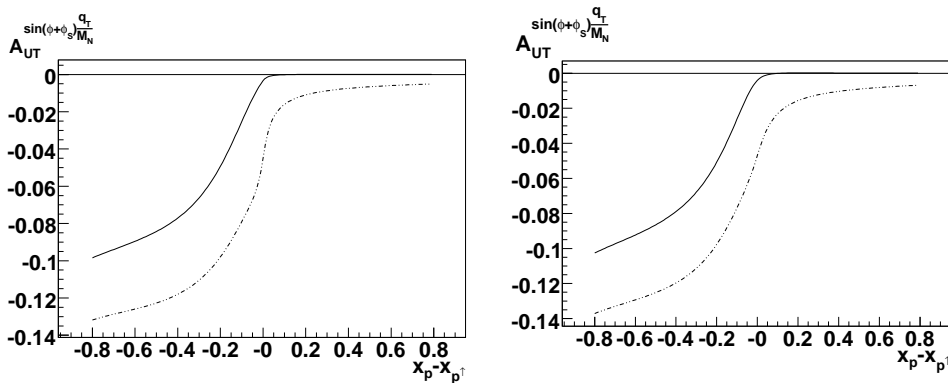


Figure 3: Estimation of SSA $A_{UT}^{\sin(\phi+\phi_S)\frac{q_T}{MN}} \Big|_{pp\uparrow}$ for RHIC, $s = 200^2 \text{ GeV}^2$, with $Q^2 = 4 \text{ GeV}^2$ (left) and $Q^2 = 20 \text{ GeV}^2$ (right). The solid and dotted curves correspond to the two different input ansatzes for h_{1u} which are used in evolution model. These are $h_{1q,\bar{q}} = \Delta q, \bar{q}$ and $h_{1q} = (\Delta q + q)/2$ $h_{1\bar{q}} = (\Delta\bar{q} + \bar{q})/2$, respectively. Here GRV94 [24] parametrization for $q(x)$ and GRSV95 [42] parametrization for $\Delta q(x)$ are used.

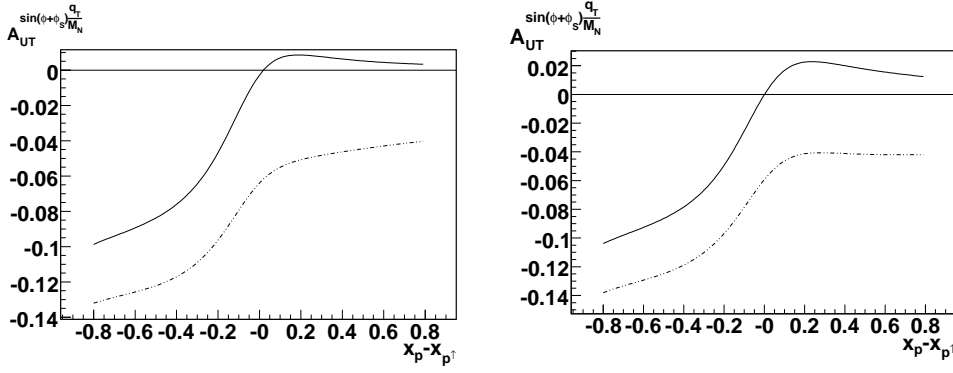


Figure 4: Estimation of SSA $A_{UT}^{\sin(\phi+\phi_S)\frac{q_T}{M_N}}|_{pp^\uparrow}$ for NICA, $s = 400 \text{ GeV}^2$, with $Q^2 = 4 \text{ GeV}^2$ (left) and $Q^2 = 15 \text{ GeV}^2$ (right). The solid and dotted curves correspond to the two different input ansatzes for h_{1u} which are used in evolution model. These are $h_{1q,\bar{q}} = \Delta q, \bar{q}$ and $h_{1q} = (\Delta q + q)/2$ $h_{1\bar{q}} = (\Delta\bar{q} + \bar{q})/2$, respectively. Here GRV94 [24] parametrization for $q(x)$ and GRSV95 [42] parametrization for $\Delta q(x)$ are used.

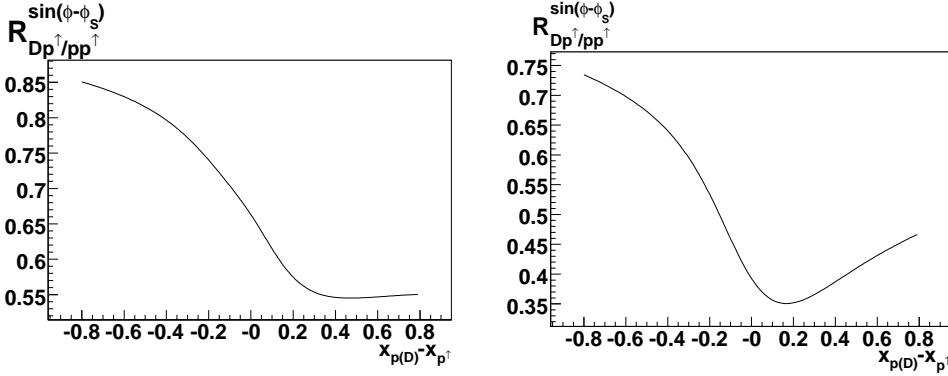


Figure 5: Estimation of ratio $R = A_{UT}^{\sin(\phi-\phi_S)\frac{q_T}{M_N}}|_{Dp^\uparrow} / A_{UT}^{\sin(\phi-\phi_S)\frac{q_T}{M_N}}|_{pp^\uparrow}$ for NICA kinematics with $Q^2 = 4 \text{ GeV}^2$ (left) and $Q^2 = 15 \text{ GeV}^2$ (right).

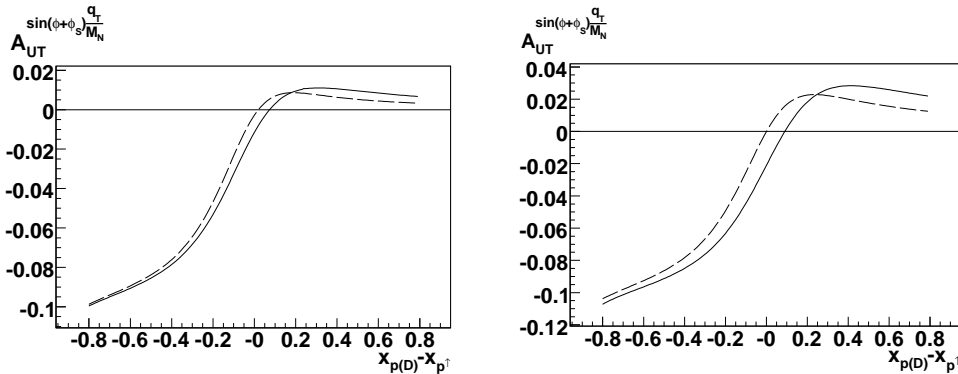


Figure 6: Estimation of SSA $A_{UT}^{\sin(\phi+\phi_S)\frac{q_T}{M_N}}$ for NICA with two different options, pp^\uparrow (dashed line) and Dp^\uparrow (solid line) collisions, with $Q^2 = 4 \text{ GeV}^2$ (left) and $Q^2 = 15 \text{ GeV}^2$ (right). Here evolution model for h_{1q} is used with the input ansatz $h_{1q,\bar{q}} = \Delta q, \bar{q}$. GRV94 [24] for q and GRSV95 [42] parametrizations for Δq are used.

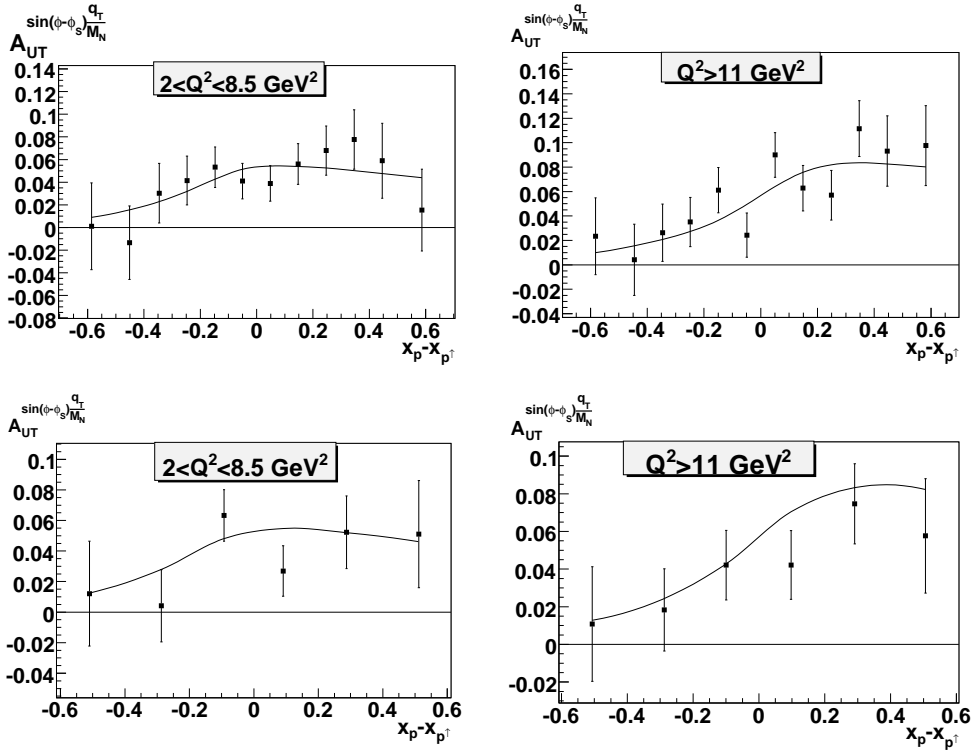


Figure 7: Estimation of asymmetries $A_{UT}^{\sin(\phi-\phi_S)\frac{q_T}{M_N}}|_{pp\uparrow}$ for NICA, $s = 400\text{GeV}^2$. Here fit from Ref. [8] is used. The points with error bars are obtained by using simulations with event generator at the applied statistics 100K pure Drell-Yan events. $\langle Q^2 \rangle \simeq 3.5\text{GeV}^2$ and $\langle Q^2 \rangle = 15\text{GeV}^2$ for the left and right plots, respectively.

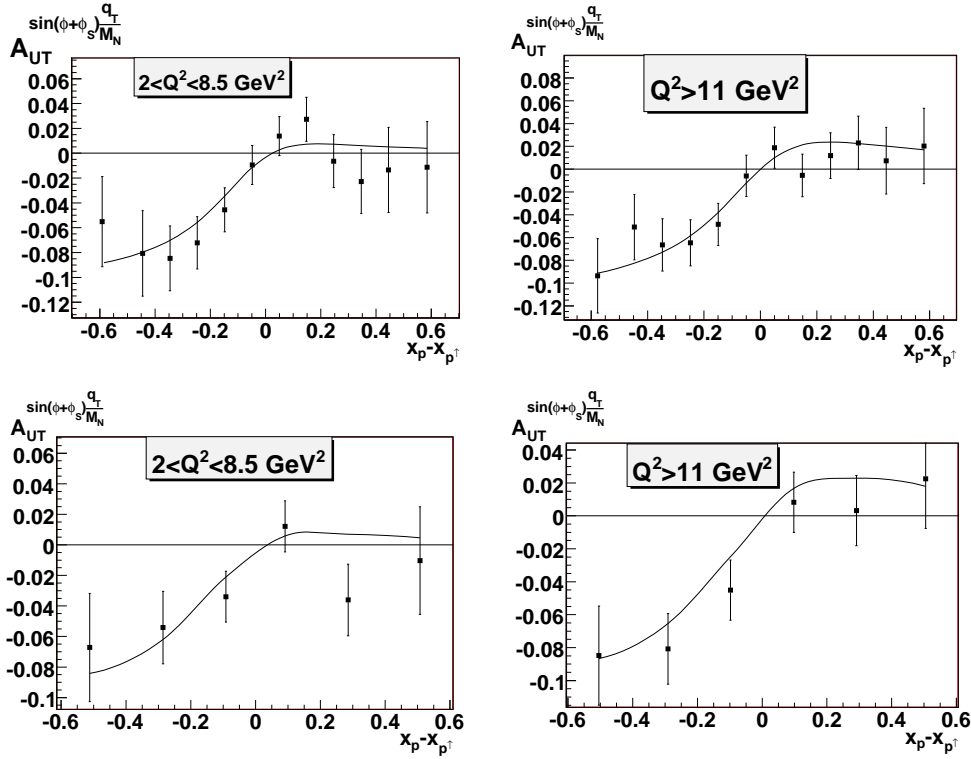


Figure 8: Estimation of asymmetries $A_{UT}^{\sin(\phi+\phi_S)\frac{q_T}{M_N}} \Big|_{pp\uparrow}$ for NICA, $s = 400\text{GeV}^2$. Here the evolution model with the input ansatz $h_{1q,\bar{q}} = \Delta q, \bar{q}$ at $Q_0^2 = 0.23\text{GeV}^2$ is used. GRV94 [24] parametrization for $q(x)$ and GRSV95 [42] parametrization for $\Delta q(x)$ are used. The points with error bars are obtained with the developed generator of polarized DY events at the applied statistics 100K (top) and 50K (bottom) pure Drell-Yan events. $\langle Q^2 \rangle \simeq 3.5\text{GeV}^2$ and $\langle Q^2 \rangle = 15\text{GeV}^2$ for the left and right plots, respectively.

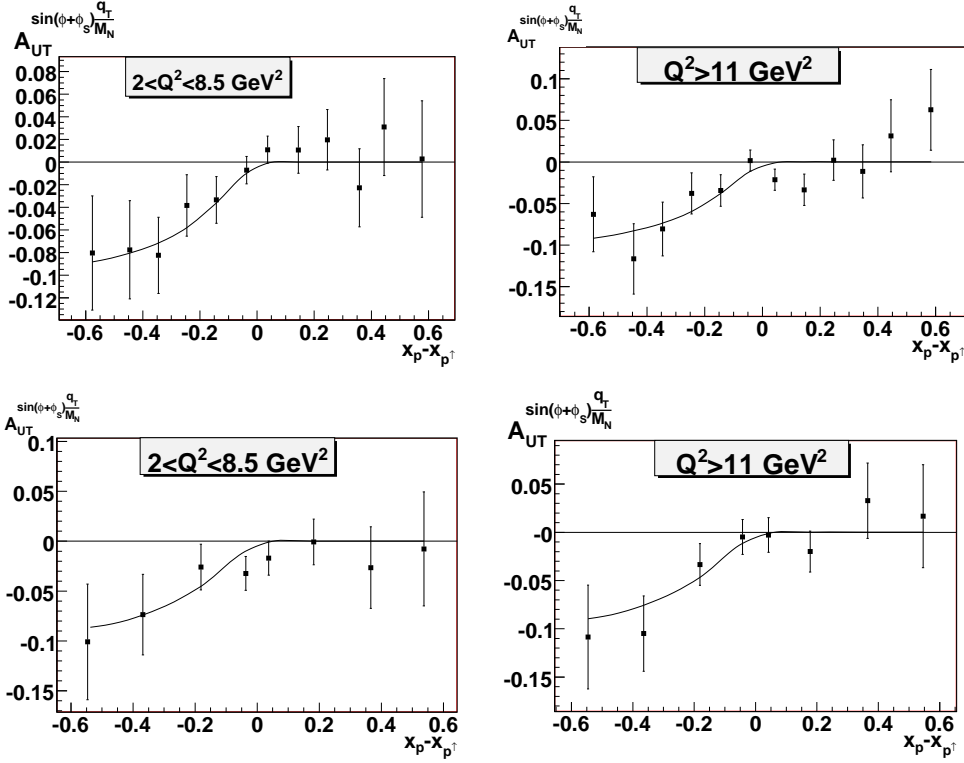


Figure 9: Estimation of asymmetries $A_{UT}^{\sin(\phi+\phi_S)\frac{q_T}{M_N}} \Big|_{pp\uparrow}$ for RHIC, $s = 200^2 GeV^2$. Here the evolution model with the input ansatz $h_{1q,\bar{q}} = \Delta q, \bar{q}$ at $Q_0^2 = 0.23 GeV^2$ is used. GRV94 [24] parametrization for $q(x)$ and GRSV95 [42] parametrization for $\Delta q(x)$ are used. The points with error bars are obtained with the developed generator of polarized DY events at the applied statistics 100K (top) and 50K (bottom) pure Drell-Yan events. $\langle Q^2 \rangle \simeq 3.9 GeV^2$ and $\langle Q^2 \rangle = 22 GeV^2$ for the left and right plots, respectively.

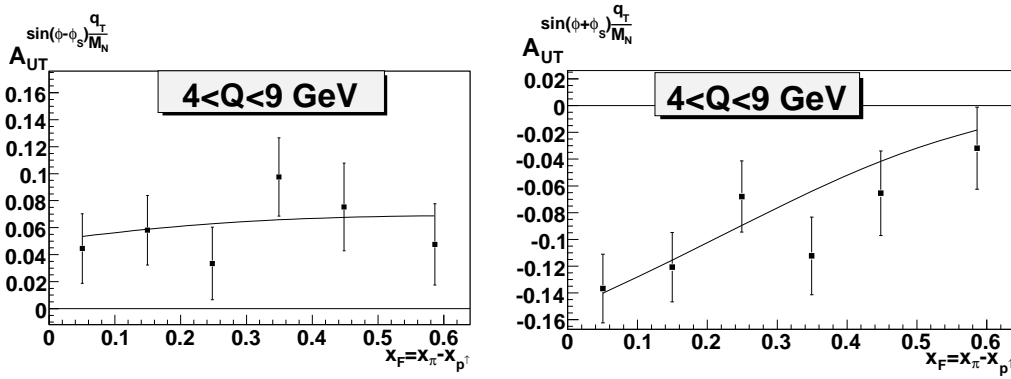


Figure 10: Estimations on SSA $A_{UT}^{\sin(\phi-\phi_S)\frac{q_T}{M_N}}|_{\pi^-p^\uparrow}$ (left) and $A_{UT}^{\sin(\phi+\phi_S)\frac{q_T}{M_N}}|_{\pi^-p^\uparrow}$ (right) feasibility for COMPASS, $s = 300 \text{ GeV}^2$. Magnitude of $A_{UT}^{\sin(\phi+\phi_S)\frac{q_T}{M_N}}|_{\pi^-p^\uparrow}$ (solid curve) is estimated just as in Ref. [22] (see discussion on Figs. 3 and 4 in Ref. [22]). For estimation of $A_{UT}^{\sin(\phi-\phi_S)\frac{q_T}{M_N}}|_{\pi^-p^\uparrow}$ (solid curve) fit from [8] for $f_{1T}^{\perp(1)q}|_{p^\uparrow}$ and parametrization [43] on $f_{1q}|_{\pi^-}$ are used. The points with error bars are obtained with the developed generator of polarized DY events at the applied statistics 50K pure Drell-Yan events. $\langle Q^2 \rangle \simeq 25 \text{ GeV}^2$ for both plots.